Carbon monoxide adsorption and dissociation on Mn-decorated Rh(1 1 1) and Rh(5 5 3) surfaces: A first-principles study

Xiufang Ma [a,b], Hai-yan Su [a], Huiqiu Deng [c], Wei-Xue Li [a,*]

[a] State Key Laboratory of Catalysis, and Center for Computational and Theoretical Chemistry, Dalian Institute of Chemical Physics, Chinese Academy of Sciences, Zhongshan Road 457, Dalian, Liaoning 116023, China
[b] Graduate School of the Chinese Academy of Sciences, Beijing 100039, China
[c] Department of Applied Physics, College of Physics and Microelectronics Science, Hunan University, Changsha 410082, China

ARTICLE INFO

ABSTRACT

Efficient CO activation on Rh particles promoted by Mn cocatalysts is important to the activity for the conversion of the syngas (CO and H_2) to hydrocarbon and oxygenates. To study the effect of the step edge and promotion of Mn cocatalysts on CO activation, we studied the CO dissociation on Mn-decorated Rh(1 1 1) and stepped Rh(5 5 3) surfaces using density functional theory calculations. We found that the presence of the step edge and Mn stabilizes the transition state and reaction products: compared to clean Rh(1 1 1), calculated barrier for CO dissociation on Mn-decorated Rh(5 5 3) is lowered by about 1.60 eV, and corresponding reaction energies with respect to CO in gas phase changes from endothermic (0.21 eV) to strong exothermic (−1.73 eV). The present work indicates that the addition of Mn cocatalysts and decrease of Rh particle sizes improves greatly the activity of CO dissociation.

1. Introduction

Synthesis gas (CO and H_2) reforming from coal, gas or biomass is rapidly growing in importance as a source of ultra-clean liquid energy fuels and valuable raw chemicals. For example, the high quality of the diesel fuel with a little sulfur/(poly) aromatics and high cetane number can be obtained via Fischer–Tropsch synthesis (FTS) [1]. In addition, selective conversion of the syngas towards various petrochemicals and raw chemicals such as short chain olefins and oxygenates (alcohols, carboxylic acids, ethers, etc.), provides an alternative and oil-independent supply for the important solvent and polymer industries [2]. Fundamental understanding to reaction mechanism is therefore required to design the catalysts with better activity and selectivity. The reaction involves an intricate reaction network composed of tremendous intermediates and elementary reaction pathways, such as CO activation, hydrogenation of carbon-containing species and oxygen, hydrocarbon chain growth, and CO insertion (oxygenates). These are still challenge in the field, and attract extensive efforts from both of experimental [3–10] and theoretical [11–13] point of views. Among them the addition of promoters/cocatalysts receives particularly attention [14–17]. In general, efficient CO adsorption and activation on the catalysts is essential to the activity and selectivity of the syngas

conversion. On noble transition metals (TMs) (such as Pt, Pd, and Cu), in which the carbon–oxygen bond breaking is prohibited, the formation of the methanol via hydrogenation is preferred [18–22]. On the other hand, on highly active TMs such as Ru, Fe, Co and Ni, in which carbon–oxygen bond breaking is facile [1,23–28], the selectivity towards the hydrocarbons is high. For the catalysts with modest activity (such as Rh), there are considerable CO molecules remained on the catalysts, and the selectivity of various oxygenates is considerable [29,30].

Rh catalysts with modest activity for CO activation is widely used as a catalyst for selective conversion of the syngas to C_n-oxygenates ($n \geq 2$, such as acetic acid, ethanol, and acetaldehyde) [30–37]. Typically Mn is added to improve the performance of Rh catalysts [38–44]. Despite the numerous studies, the detail mechanism for the promotion of Mn on the reactivity of Rh catalysts for this process remains unclear. Knözinger et al. [45] and Ichikawa et al. [46,47] proposed that the addition of Mn enhances CO dissociation through the formation of a tilted CO adsorbed at the Rh–Mn interface. In this case, the existence of the second metal creates the favorable sites for C and O adsorption (bifunctional effect), thus lead to the reduction of the barrier for CO dissociation. Whereas van den Berg et al. [48] suggest that the presence of Mn modifies the electronic properties of the catalysts (ligand effect). As a result, CO adsorption was weakened thus free more sites for H adsorption and the reaction rate increases accordingly. Fierro et al. [49] found that Mn promoter behaved as an electron-withdrawing, partially oxidizing the Rh

* Corresponding author. Tel.: +86 411 84379996.
  E-mail address: wxli@dicp.ac.cn (W.-X. Li).

atoms at the Rh–MnO interface and creating new sites for CO insertion.

To shed light on the promotion of Mn on Rh catalysts for CO activation, which is related to the activity and selectivity of syngas conversion, we represent here a DFT study on CO dissociation on monometallic and Mn modified Rh surfaces. To illustrate of the defect effects of Rh nanoparticles, we studied the Rh surface with and without the presence of step edge. Because the CO activation is elementary process for syngas conversion, the results and insights obtained may be of general interest. The paper remained is organized as follows. The calculation methods are described in Section 2. The main results including CO adsorption and dissociation on Rh(1 1 1) and Rh(5 5 3) alloyed with Mn are presented in Section 3. The origin of the promotion of Mn and step edge on CO activation is discussed in Section 4. Finally, the conclusions are summarized.

2. Computational details

All calculations were performed using plane wave code DACAPO [50], in which ultrasoft pseudo potentials were used to describe the ionic cores [51]. The Kohn–Sham one-electron valence states were expanded in a basis of plane waves with kinetic energy 340 eV and density cutoff 400 eV. The self-consistent density was determined by iterative diagonalization of the Kohn–Sham Hamiltonian with Fermi population of the Kohn–Sham states ($k_BT = 0.1$ eV) and Puly mixing of the resulting electronic density. The exchange-correlation energy and potential were described by generalized gradient approximation in form of revised Perdew–Burke–Ernzerhof (RPBE), which was reported to give better description of the adsorption energies [50]. When Mn atoms were involved, spin-polarized calculations were performed without statement otherwise. The calculated lattice constant for bulk Rh is 3.84 Å, which agrees well with the experiments (3.80 Å) [52], and was used in present work.

To simulate (1 1 1) surface, a five layer (2×2) slab periodically repeated in a super cell geometry with seven equivalent layers of vacuum was used. The surface Brillouin zone was sampled by ($4 \times 4 \times 1$) Monkhorst–Pack grid [53]. The RhMn(1 1 1) surface alloy (Fig. 1a) was used to study of the promotion of Mn on the activity, and preliminary study was reported in earlier study [54]. Adsorbates and atoms in top two metal layers were optimized till the residual forces less than 0.02 eV/Å. The stepped Rh(5 5 3) surface consists of five-atom-wide (1 1 1) terraces separated by monatomic (1 1 1)-faceted steps, approximately 10 Å apart as shown in Fig. 1b. The surface was simulated by a slab with five equivalent (1 1 1) layers. The stepped surfaces were separated by 15 Å vacuum, and the atoms in the uppermost layer parallel to the (1 1 1) and the adsorbates were relaxed till the residual forces less than 0.05 eV/Å. The Brillouin zone integration has been performed using a ($4 \times 2 \times 1$) Monkhorst–Pack grid. A one-dimensional Mn chain along step edge was used to study the possible promotion of Mn on CO activation.

CO molecule was placed on the unconstrained side of the surfaces, and a posterior dipole correction was applied in the normal direction of the surface [55]. Spin-polarization calculations for isolated molecules and atoms in gas phase were carried out in a (12.1 Å $\times 12.2$ Å $\times 12$ Å) unit cell with single k-point. The calculated gas phase CO bond length is 1.14 Å, and agrees well with the experimental value of 1.13 Å [56]. The binding energy of the molecule E_b was calculated with respect to the energy gain of the adsorption on the clean surfaces. Here a negative (positive) value indicates that the adsorption is exothermic (endothermic).

The transition states (TSs) of the reactions were searched by constraining the reaction coordinate of the reactants at different values with incremental step of 0.1 Å but optimizing remained degrees of freedom simultaneously. Near the TS, the variation of the reac-
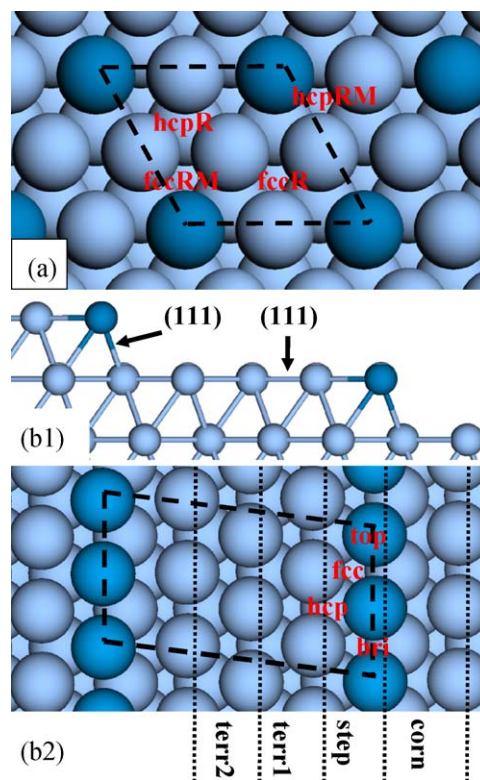
Fig. 1. The adsorption sites for molecular adsorption on RhMn(1 1 1) surface alloys (top view) (a), and RhMn(5 5 3) (b1 for side view and b2 for top view). Silver white balls represent Rh atoms, and blue balls for Mn or step atoms. "Step", "terr1", "terr2", and "corn" correspond different regions on vicinal Rh surfaces. The unit cells used in calculation are indicated. (For interpretation of the references to color in this figure legend, the reader is referred to the web version of the article.)

tion coordinates was decreased to 0.01 Å so that the TS could be determined accurately [57,58] and further verified by frequency analysis.

3. Results

3.1. Rh(1 1 1) surface

We first studied CO, atomic C and O adsorption on Rh(1 1 1). As listed in Table 1, CO, C and O prefers to adsorb at top, fcc, and hcp sites with the binding energies of −1.77 eV, −6.89 eV and −4.66 eV with respect to CO, atomic C and O in gas phase, respectively. For C and O coadsorption (the product from CO dissociation), the most favorable configuration is that C adsorbs at the hcp site and O at the fcc site over a Rh atom. Compared to CO in gas phase, this configuration is endothermic by 0.21 eV. Corresponding reaction diagram is indicated in Fig. 2. At the TS, carbon atom sits at the hollow site, while oxygen atom at the bridge site nearby as indicated in Fig. 3a. The calculated C–O bond length 1.87 Å is stretched greatly compared to that of CO in gas phase 1.14 Å. This suggests that the TS is late transition state and product-like. The elemen-

Table 1
Binding energies (unit: eV/atom) for CO, atomic C, and O (0.25 ML) at preferential sites on Rh(1 1 1) and RhMn(1 1 1) surface. The energies reference is CO, atom C and O in gas phase.

|	CO		C		O	
	Site	Energy	Site	Energy	Site	energy
Rh(1 1 1)	Top	−1.77	Hcp	−6.89	Fcc	−4.66
RhMn(1 1 1)	HcpR	−1.88	HcpR	−7.15	FccRM	−4.97
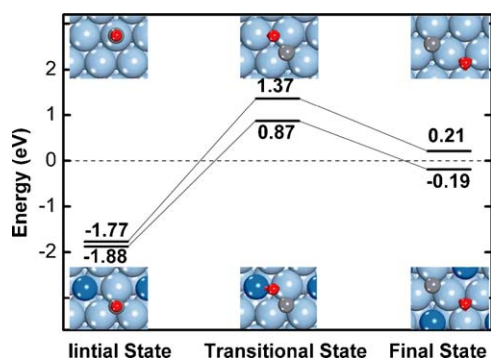
Fig. 2. Potential energy diagram for CO dissociation on Rh(1 1 1) (upper line) and RhMn(1 1 1) (lower line). Structures at the initial state, transition state, and final state are shown schematically, and the energy reference (eV) is CO in gas phase.

tary reaction energy is 1.98 eV (strongly endothermic) with respect to the adsorbed CO and the corresponding activation energy is 3.14 eV. The large activation barrier for CO dissociation, compared to CO binding energy (−1.77 eV), indicates the rather low activity for CO dissociation on Rh(1 1 1). These agree well with Mavrikakis and co-workers's calculations (E_a = 3.14 eV) [59], and experimental observations [60], where CO dissociation does not occur on Rh foil at temperatures of 400 K.

3.2. RhMn(1 1 1) surface alloy

In past, we studied the molecule adsorption on RhMn(1 1 1) surface alloy [54]. We found that in the presence of atomic oxygen, RhMn surface alloy is energetically most favorable compared to Mn substitutional adsorption in the Rh(1 1 1) subsurface and bulk region, because of oxygen induced segregation from strong interaction between oxygen and Mn. Accordingly, we focused on CO
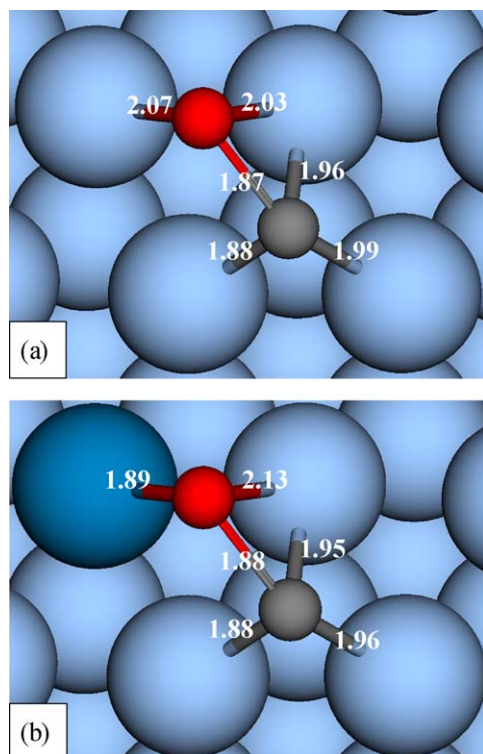
Fig. 3. The optimized transition state for CO dissociation on Rh(1 1 1) (a) and RhMn(1 1 1) (b), and the unit is Å.

Table 2
Binding energies (unit: eV/atom) for CO, atomic C and O (0.10 ML) at different area and sites of Rh(5 5 3). The energies reference is CO, atomic C and O in gas phase.

Site	CO	C	O
Step[a]			
Top	−1.83		
Fcc	−1.76	−6.67	−4.76
Hcp	−1.71	−6.94	−4.51
Bridge	−1.81	−6.49	−4.87
Corn[a]			
Top	−1.59		
Fcc	−1.39	−6.36	−4.21
Hcp	−1.59	−7.14	

[a] Step and corn correspond to the different area of Rh(5 5 3), as indicated in Fig. 1b.

dissociation on RhMn(1 1 1) surface alloy. A brief summary for CO, C and O adsorption on RhMn(1 1 1) surface alloy from reference [54] was presented in Table 1. We found that that CO and C prefer to coordinate Rh atoms and adsorb at so-called hcpR site as indicated in Fig. 1a. The corresponding binding energies are −1.88 and −7.15 eV, respectively. Whereas, atomic oxygen prefers to coordinate with Mn due to its strong oxophilicity and calculated binding energy is −4.97 eV. Compared to Rh(1 1 1), the interaction between molecules and RhMn(1 1 1) surfaces are enhanced in general by 0.3 eV due to the electronic effect induced by Mn, as discussed later. For the C and O coadsorption, the most stable configuration is that the atomic C sits in the hcp site and the atomic O in the fcc hollow site over the Rh atom, and the corresponding energy is −0.19 eV with respect to CO in gas phase.

The transition state for CO dissociation is similar to Rh(1 1 1) except oxygen atom coordinates with Mn and Rh at the TS, instead of two Rh atoms on Rh(1 1 1), as indicated in Fig. 3a and b. For CO dissociation on Rh(1 1 1) and RhMn(1 1 1) surfaces, C–O bond may be broken over single Rh atom, however, our calculations show that the reaction path is kinetically unfavorable and therefore not shown here. These agree well with previous DFT studies [61]. Calculated potential energy surfaces and structures are plotted in Fig. 2. At the TS (Fig. 3b), the C–O bond length is 1.88 Å. The C atom is slightly off from the hcp site, and the bond length of bridge O are 2.13 Å (Rh–O) and 1.89 Å (Mn–O), respectively. The optimized TS on both Rh(1 1 1) and RhMn(1 1 1) surfaces are similar, and consistent with the rules proposed by Michaelides and Hu [62,63], namely, the higher valency the adsorbate (e.g., carbon), the higher coordination sites (e.g., 3-fold hcp site) it occupies. Compared to the Rh(1 1 1), the barrier for CO dissociation decreases by about 0.4 eV due to the strong interaction between oxygen and Mn at the TS.

3.3. Stepped Rh(5 5 3) surface

The coordinate unsaturated sites at the step often act as the active sites for catalytic reactions [64–68] because of its high reactivity from the electronic effect (the high lying d-band center) and the geometric effect. We studied CO activation on Rh(5 5 3) (Fig. 1b) surfaces. The binding energies for CO, atomic C and O adsorption at favorable sites are listed in Table 2. CO tends to sit at top/step and bridge/step sites (Fig. 1b) with binding energy of −1.83 and −1.81 eV, respectively. C atom prefers to adsorb at hcp/corn sites with energy of −7.14, and 0.20 eV higher at hcp/step sites. For atomic oxygen, it prefers to adsorb at bridge/step with energy of −4.87 eV.

For C and O coadsorption on Rh(5 5 3) surface, we studied three possible configurations: (a) C sits at fcc/corn and O at bri/step, (b) C atom at hcp/corn and O at bridge/step, and (c) C at hcp/corn and O at fcc/step. Corresponding energies with respect to CO in gas phase are −0.28, −0.96, and −1.07 eV, respectively. Since the last one is ener-
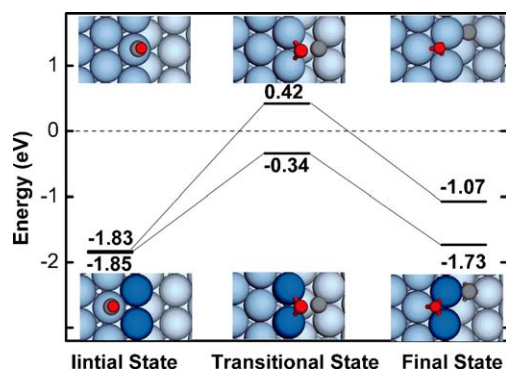
Fig. 4. Potential energy diagram for CO dissociation on Rh(5 5 3) (upper line) and RhMn(5 5 3) (lower line). Structures at the initial state, transition state, and final state are shown schematically, and the energy reference (eV) is CO in gas phase.

getically most favorable, and corresponding energetics was used as the energy of the final products from CO dissociation.

Two favorable TSs for CO dissociation were identified. Oxygen atom sits at the bridge/step sites, and carbon atom locates either at the fcc/corn sites (path I shown in Fig. 5a), or at the hcp/corn sites (path II, shown in Fig. 5b). Calculated barriers for two pathways (2.25 eV for path I and 2.27 eV for path II with respect to adsorbed CO) are very close, and both of them (Fig. 4) are lowered by about 0.90 eV than that of Rh(1 1 1). In addition, the overall reaction energy for CO dissociation on Rh(5 5 3) is −1.07 eV (exothermic) with respect to CO in gas phase, but remain endothermic with energy of 0.76 eV with respect to adsorbed CO.
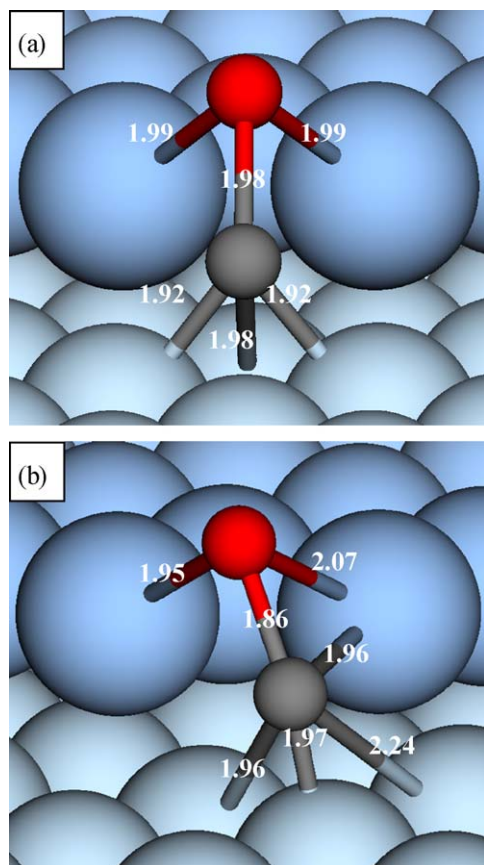
Fig. 5. The optimized transition state for CO dissociation on Rh(5 5 3) via path I (a) and path II (b), and the unit is Å.

Table 3
Binding energies (unit: eV/atom) for CO, C, and O (0.10 ML) at different area and sites of RhMn(5 5 3). The energies reference is CO, atomic C and O in gas phase.

Site	CO	C	O
Step[a]			
Fcc		−6.16	−5.63
Hcp		−6.63	−4.99
Bridge			−5.56
Corn[a]			
Top	−1.64		
Fcc	−1.53	−6.48	−4.31
Hcp	−1.56	−6.98	−4.23
Terr1[a]			
Top	−1.85		
Fcc	−1.69	−6.70	−4.70
Hcp	−1.79	−6.94	−4.61
Bridge	−1.74		
Terr2[a]			
Top	−1.77		
Fcc	−1.70	−6.72	−4.64
Hcp	−1.75	−6.90	−4.53
Bri	−1.70		

[a] Step, corn, terr1 and terr2 correspond to the different region of RhMn(5 5 3) indicated in Fig. 1.

At the transition states (shown in Fig. 5), the C atom is slightly off from the hcp sites, the C–Rh bond length is 1.92, 1.92 and 1.98 Å, respectively. The O atom coordinates with two step Rh atoms with bond length of 1.99 Å. The calculated C–O bond length at the TS is 1.98 Å, stretched significantly than that of adsorbed CO again.

3.4. RhMn(5 5 3) surface

For Mn adatom adsorbed on Rh(5 5 3) surfaces, we found that it prefers to adsorb at the step edge, and forms one-dimensional chain along the step edge. Compared to formation of surface alloys in terrace, the formation of 1D Mn chain is energetically lowered by 0.17 eV/Mn adatom. Correspondingly, we used 1D Mn chain along the step edge of Rh(5 5 3) to study the effect of Mn-promoted Rh(5 5 3) on CO dissociation.

The energetic most favorable adsorption sites and corresponding energetics for CO, atomic C and O adsorption are listed in Table 3. We found that CO adsorbs exclusively on the Rh terrace without coordination with Mn atoms, and prefers to adsorb at the top sites on the terrace (top/terr1) with the energy of −1.85 eV. For atomic carbon, the most favorable configuration is the hcp/corn sites with energy of −6.98 eV, which is 0.16 eV higher than similar sites on the Rh(5 5 3). While for atomic O, the most favorable adsorption site is the fcc/step sites with the energy of −5.63 eV, considerably stable than that of Rh(1 1 1), RhMn(1 1 1) surface alloy and Rh(5 5 3), due to the high oxophilicity of Mn at the step edge. For C and O coadsorption, the favorable configuration is that C and O sits at the hcp/corn and the fcc/step site, respectively, and the corresponding energy is −1.73 eV with respect to CO in gas phase.

Similar to Rh(5 5 3), there are two possible reaction pathways for CO dissociation on RhMn(5 5 3), and the corresponding transition states are shown in Fig. 6. Similar to Rh(5 5 3), both reaction pathways have similar activation energies (1.51 eV (Fig. 6a) and 1.55 eV (Fig. 6b)). Contrast to Rh(5 5 3), the activation energies on RhMn(5 5 3) surfaces decreases by about 0.74 eV (Fig. 4). The reaction energy becomes strongly exothermic with the energy of −1.73 eV with respect to the gas phase CO, and becomes thermal neutral even compared to adsorbed CO.

At the transition state (Fig. 6a), the C–O bond is stretched to 1.97 Å, similar to that of Rh(5 5 3). The C atom coordinates with three Rh atoms at corner with bond length of 1.93, 1.93 and 1.97 Å,
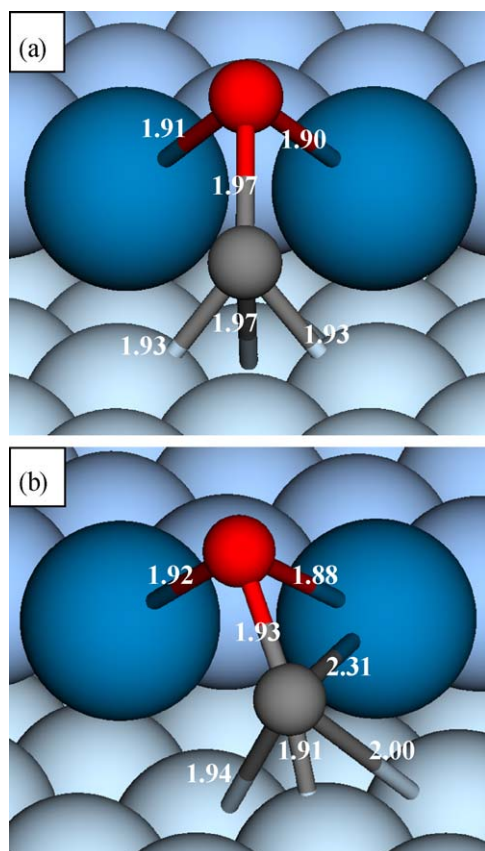
Fig. 6. The optimized transition state for CO dissociation on Mn-decorated Rh(5 5 3) via path I (a) and path II (b), and the unit is Å.

and the O atoms coordinates with two steps Mn with bond length of 1.90 Å and 1.91 Å, respectively.

4. Discussion

The origin of the promotion of Mn and step edge on the activity comes from the electronic and ensemble effect, as discussed below. First, we note that the d-band center of surface Rh atoms in the presence of Mn shifts upward for instance from −2.03 eV for Rh(1 1 1) to −1.96 eV for RhMn(1 1 1). In addition, the d-band center for step Rh atoms shifts upward to −1.87 eV. Correspondingly, the reactivity of Rh atoms due to the presence of Mn and step edge increases based on the d-band theory, as found in Tables 1–3. Meanwhile, we found that Rh tends to coordinate with CO and C, which are structure less sensitive. Furthermore, it can be seen that for CO adsorption at favorable sites on four surfaces considered, the calculated binding energies are very close (difference less than 0.11 eV) because of similar local configuration (Rh-top). Though the variation of the binding energies of carbon atom at favorable sites increases slightly in magnitude of 0.26 eV, it remains modest. In contrast, oxygen atom tends to coordinate with Mn (oxophilic) and structure sensitive. Compared to O/Rh(1 1 1) with binding energy of −4.66 eV, the binding energy of O increases to −4.97 eV by coordinating with one Mn atom on RhMn(1 1 1) and −5.63 eV by coordinating with two step Mn atoms on RhMn(5 5 3).

Since O adsorption is structure sensitive compared to CO and C, the reaction energy for CO dissociation depends sensitively on the energetics of dissociated atomic oxygen. In addition, compared to flat surface (Fig. 2), the special geometry at the step edge (ensemble effect) minimizes greatly the site competition between dissociated C and O (Fig. 4), and stabilizes the overall energetics further. As a
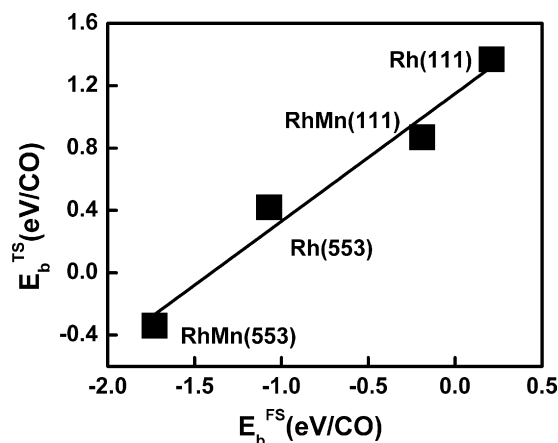
Fig. 7. Energetics for CO dissociation at the favorable transition states of (E_b^{TS}) versus the final states (E_b^{FS}) on four surfaces considered. The energy reference (eV) is CO in gas phase.

consequence, calculated reaction energies for CO dissociation with respect to CO in gas phase are 0.21, −0.19, −1.07 and −1.73 eV for Rh(1 1 1), RhMn(1 1 1), Rh(5 5 3) and RhMn(5 5 3), respectively. The overall effects from Mn and step are dramatic and corresponding reaction energetics varies in magnitude of 2 eV. On RhMn(5 5 3) surfaces, CO dissociation becomes even thermal neutral with respect to adsorbed CO.

The improved reaction energetics also affects the corresponding kinetics. Compared to elementary activation energy 3.14 eV (with respect to adsorbed CO) for CO dissociation on Rh(1 1 1), it decreases to 2.75, 2.25 and 1.51 eV on RhMn(1 1 1), Rh(5 5 3) and RhMn(5 5 3) surfaces, respectively. The trend follows exactly the variation of the reaction energetics. To see this clearly, the elementary activation energies is plotted with respect to the energetics of the final states, and shown in Fig. 7. All activation barriers and the energetics of the final states plotted are referred to CO in gas phase, as indicated in Figs. 2 and 4. A nice linear correlation between activation barriers and the energetics of the final states can be found. The reason for the linear correlation comes from the fact that the transition states for CO dissociation are a late transition state and CO adsorption is structure insensitive. Accordingly, the barrier for CO dissociation is completely determined by the energetics of the final states.

Above analysis show that decrease of the Rh particle sizes and addition of Mn cocatalysts would improve considerably not only the overall energetics but also the kinetics for CO dissociation at the Rh–Mn interfaces. Knözinger et al. [45] and Ichikawa et al. [46,47] proposed that CO dissociation can be enhanced through the formation of a tilted mode of CO adsorbed at the Rh–Mn interface, which could be rationalized by the present calculations. Under the realistic conditions, Mn is, however, not in metallic state and actually partially oxidized. Therefore, the extent of the promotion of Mn on CO dissociation from the present calculation could be overestimated. On the other hand, we note that it has been reported that the presence of hydrogen may promote CO dissociation on Co [11], Fe [69] and Ru [70], but not discussed here either. Further theoretical studies for CO dissociation on Rh catalysts with presence of oxidic Mn and hydrogen are required.

5. Conclusion

In summary, we studied CO dissociation on Mn-decorated Rh(1 1 1) and Rh(5 5 3) surfaces using first-principles density functional theory calculations. Independent on the surfaces considered, we found that the CO dissociation is a late transition state-like. The

activation barrier for C–O bond breaking is determined by the energetics of the products, and there is a linear correlation between the activation barriers and the energetics of the products. For CO dissociation, we found that the presence of Mn and step edge improves dramatically not only the kinetics but also the energetics. These indicate that the activity for syngas conversion could be promoted by decrease of Rh particle sizes and the addition of Mn cocatalysts.

Acknowledgments

References

[1] E. Iglesia, Appl. Catal. A 161 (1997) 59.
[2] A. Martínez, G. Prieto, Top. Catal. 52 (2009) 75.
[3] M. Bwoker, Catal. Today 15 (1992) 77.
[4] J.T. Kummer, P.H. Emmett, J. Am. Chem. Soc. 75 (1953) 5177.
[5] H. Orita, S. Naito, K. Tamaru, J. Catal. 90 (1984) 183.
[6] S.D. Jackson, B.J. Brandreth, D. Winstanley, J. Catal. 106 (1987) 464.
[7] T.L.F. Favre, L. Gerrit van der, P. Vladimir, J. Chem. Soc., Chem. Commun. (1985) 230.
[8] M.K. Carter, J. Mol. Catal. A: Chem. 172 (2001) 193.
[9] R.C. Brady, R. Pettit, J. Am. Chem. Soc. 103 (1981) 1287.
[10] C.K. Rofer-DePoorter, Chem. Rev. 81 (1981) 447.
[11] O.R. Inderwildi, S.J. Jenkins, D.A. King, J. Phys. Chem. C 112 (2008) 1305.
[12] Y. Choi, P. Liu, J. Am. Chem. Soc. 131 (2009) 13054.
[13] J. Cheng, P. Hu, P. Ellis, S. French, G. Kelly, C.M. Lok, J. Phys. Chem. C 112 (2008) 6082.
[14] H.Y. Luo, W. Zhang, H.W. Zhou, S.Y. Huang, P.Z. Lin, Y.J. Ding, L.W. Lin, Appl. Catal. A 214 (2001) 161.
[15] B.J. Kip, P.A.T. Smeets, J. van Grondelle, R. Prins, Appl. Catal. 33 (1987) 181.
[16] H. Arakawa, T. Fukushima, M. Ichikawa, S. Natsushita, K. Takeuchi, T. Matsuzaki, Y. Sugi, Chem. Lett. 14 (1985) 881.
[17] W.M.H. Sachtler, D.F. Shriver, W.B. Hollenberg, A.F. Lang, J. Catal. 92 (1985) 429.
[18] B. Hu, Y. Yamaguchi, K. Fujimoto, Catal. Commun. 10 (2009) 1620.
[19] X.-M. Liu, G.Q. Lu, Z.-F. Yan, J. Beltramini, Ind. Eng. Chem. Res. 42 (2003) 6518.
[20] Y. Ma, Q. Ge, W. Li, H. Xu, Appl. Catal. B: Environ. 90 (2009) 99.
[21] Y. Matsumura, W.-J. Shen, Y. Ichihashi, M. Okumura, J. Catal. 197 (2001) 267.
[22] W.J. Shen, Y. Ichihashi, M. Okumura, Y. Matsumura, Catal. Lett. 64 (2000) 23.
[23] A.Y. Khodakov, W. Chu, P. Fongarland, Chem. Rev. 107 (2007) 1692.
[24] M.E. Dry, Catal. Today 71 (2002) 227.
[25] H. Schulz, Appl. Catal. A 186 (1999) 3.
[26] J.J.C. Geerlings, J.H. Wilson, G.J. Kramer, H.P.C.E. Kuipers, A. Hoek, H.M. Huisman, Appl. Catal. A 186 (1999) 27.
[27] A.A. Adesina, Appl. Catal. A 138 (1996) 345.
[28] B. Jager, R. Espinoza, Catal. Today 23 (1995) 17.
[29] J.J. Spivey, A. Egbebi, Chem. Soc. Rev. 36 (2007) 1514.
[30] V. Subramani, S.K. Gangwal, Energy Fuels 22 (2008) 814.
[31] J. Hu, Y. Wang, C. Cao, D.C. Elliott, D.J. Stevens, J.F. White, Catal. Today 120 (2007) 90.
[32] M.M. Bhasin, W.J. Bartley, P.C. Ellgen, T.P. Wilson, J. Catal. 54 (1978) 120.
[33] M. Ichikawa, Bull. Chem. Soc. Jpn. 51 (1978) 2268.
[34] M. Ichikawa, Bull. Chem. Soc. Jpn. 51 (1978) 2273.
[35] J. Kowalski, G.V.D. Lee, V. Ponec, Appl. Catal. 19 (1985) 423.
[36] R.P. Underwood, A.T. Bell, J. Catal. 111 (1988) 325.
[37] P.Z. Lin, D.B. Liang, H.Y. Luo, C.H. Xu, H.W. Zhou, S.Y. Huang, L.W. Lin, Appl. Catal. A 131 (1995) 207.
[38] R. Burch, M.I. Petch, Appl. Catal. A 88 (1992) 39.
[39] H.-Y. Luo, P.-Z. Lin, S.-B. Xie, H.-W. Zhou, C.-H. Xu, S.-Y. Huang, L.-W. Lin, D.-B. Liang, P.-L. Yin, Q. Xin, J. Mol. Catal. A: Chem. 122 (1997) 115.
[40] N. Testuo, S. Ken-ichi, M. Shinya, A. Hironori, J. Chem. Soc., Chem. Commun. (1987) 647.
[41] K.P. De Jong, J.H.E. Glezer, H.P.C.E. Kuipers, A. Knoester, C.A. Emeis, J. Catal. 124 (1990) 520.
[42] H.T. Ma, Z.Y. Yuan, Y. Wang, X.H. Bao, Surf. Interface Anal. 32 (2001) 224.
[43] H. Treviño, W.M.H. Sachtler, Catal. Lett. 27 (1994) 251.
[44] A.G.T.M. Bastein, W.J. van Der Boogert, G. van Der Lee, H. Luo, B. Schuller, V. Ponec, Appl. Catal. 29 (1987) 243.
[45] A.S. Lisitsyn, S.A. Stevenson, H. Knözinger, J. Mol. Catal. 63 (1990) 201.
[46] W.M.H. Sachtler, M. Ichikawa, J. Phys. Chem. 90 (1986) 4752.
[47] M. Ichikawa, T. Fukushima, J. Phys. Chem. 89 (1985) 1564.
[48] F.G.A. van den Berg, J.H.E. Glezer, W.M.H. Sachtler, J. Catal. 93 (1985) 340.
[49] M. Ojeda, M.L. Granados, S. Rojas, P. Terreros, F.J. García-García, J.L.G. Fierro, Appl. Catal. A 261 (2004) 47.
[50] B. Hammer, L.B. Hansen, J.K. Norskov, Phys. Rev. B 59 (1999) 7413.
[51] D. Vanderbilt, Phys. Rev. B 41 (1990) 7892.
[52] M. Birgersson, C.O. Almbladh, M. Borg, J.N. Andersen, Phys. Rev. B 67 (2003) 045402.
[53] H.J. Monkhorst, J.D. Pack, Phys. Rev. B 13 (1976) 5188.
[54] X.F. Ma, H.Q. Deng, M.-M. Yang, W.-X. Li, J. Chem. Phys. 129 (2008).
[55] L. Bengtsson, Phys. Rev. B 59 (1999) 12301.
[56] J.A. Dean, Lange's Handbook of Chemistry, 15th edition, McGraw-Hill, 1999.
[57] H.-Y. Su, X.-H. Bao, W.-X. Li, J. Chem. Phys. 128 (2008) 194707.
[58] T.R. Munter, T. Bligaard, C.H. Christensen, J.K. Nørskov, Phys. Chem. Chem. Phys. 10 (2008) 5202.
[59] M. Mavrikakis, M. Baumer, H.J. Freund, J.K. Nørskov, Catal. Lett. 81 (2002) 153.
[60] V. Nehasil, I. Stara, V. Matolin, Surf. Sci. 331 (1995) 105.
[61] Y. Morikawa, J.J. Mortensen, B. Hammer, J.K. Nørskov, Surf. Sci. 386 (1997) 67.
[62] A. Michaelides, P. Hu, J. Am. Chem. Soc. 122 (2000) 9866.
[63] A. Michaelides, P. Hu, J. Chem. Phys. 114 (2001) 5792.
[64] G.A. Somorjai, Introduction To Surface Chemistry and Catalysis, Wiley, New York, 1994.
[65] R.I. Masel, Principles of Adsorption and Reaction on Solid Surfaces, Wiley, New York, 1996.
[66] A. Logadottir, J.K. Nørskov, J. Catal. 220 (2003) 273.
[67] J.K. Nørskov, T. Bligaard, A. Logadottir, S. Bahn, L.B. Hansen, M. Bollinger, H. Bengaard, B. Hammer, Z. Sljivancanin, M. Mavrikakis, Y. Xu, S. Dahl, C.J.H. Jacobsen, J. Catal. 209 (2002) 275.
[68] A. Stroppa, F. Mittendorfer, J.N. Andersen, G. Parteder, F. Allegretti, S. Surnev, F.P. Netzer, J. Phys. Chem. C 113 (2009) 942.
[69] C.-F. Huo, J. Ren, Y.-W. Li, J. Wang, H. Jiao, J. Catal. 249 (2007) 174.
[70] O.R. Inderwildi, S.J. Jenkins, D. King, Angew. Chem. Int. Ed. 47 (2008) 5253.